PHYSICAL REVIEW D **82,** 105012 (2010)

Non-mean-field quantum critical points from holography

Nick Evans,[1,*] Kristan Jensen,[2,†] and Keun-Young Kim[1,‡]

[1]*School of Physics and Astronomy, University of Southampton, Southampton, SO17 1BJ, UK*
[2]*Department of Physics, University of Washington, Seattle, Washington 98195-1560, USA*

(Received 20 August 2010; published 15 November 2010)

We construct a class of quantum critical points with non-mean-field critical exponents via holography. Our approach is phenomenological. Beginning with the D3/D5 system at nonzero density and magnetic field which has a chiral phase transition, we simulate the addition of a third control parameter. We then identify a line of quantum critical points in the phase diagram of this theory, provided that the simulated control parameter has dimension less than two. This line smoothly interpolates between a second-order transition with mean-field exponents at zero magnetic field to a holographic Berezinskii-Kosterlitz-Thouless transition at larger magnetic fields. The critical exponents of these transitions only depend upon the parameters of an emergent infrared theory. Moreover, the non-mean-field scaling is destroyed at any nonzero temperature. We discuss how generic these transitions are.

DOI: 10.1103/PhysRevD.82.105012 PACS numbers: 11.25.Tq

I. INTRODUCTION AND SUMMARY

The anti–de Sitter/conformal field theory (AdS/CFT) correspondence [1–3] describes a class of strongly coupled gauge theories in terms of weakly coupled gravitational systems. It has proved an extremely versatile tool for the study of strong coupling phenomena over the last ten years. For example, the correspondence has been used to study the physics of deconfined plasmas, including transport [4] and energy loss [5,6]. Recently there has been much interest in the use of AdS/CFT to realize condensed matter phenomena. Much of this work has been dedicated to the study of non-Fermi liquids [7–9] and holographic superfluids [10,11] in the hope of better understanding the phase diagram of high-temperature superconductors. Another route to the same goal involves the study of quantum critical points in strongly interacting theories. These zero temperature transitions are interesting in their own right, as they tend to govern the physics of large swaths of the phase diagram at nonzero temperature. Indeed, the ''strange metal'' phases observed in high-temperature superconductors may originate from a quantum critical point [12].

The study of critical phenomena is of central importance in the condensed matter community. At any continuous phase transition there is an emergent infrared fixed point [13]. Of particular interest are transitions where the infrared theory is itself an interacting quantum field theory. These transitions are characterized by non-mean-field critical exponents. It would be extremely interesting if holography could be used to study these transitions or perhaps even transitions beyond the Landau-Ginzburg-Wilson paradigm altogether [14]. Unfortunately, most continuous transitions in holographic models are second order with mean-field exponents [15]. In fact, the mean-field exponents should be expected rather than surprising. They appear because of the large N parameter in these theories, which allows us to study them via their holographic duals. In this limit quantum fluctuations are suppressed in both the field [16] and gravitational theories. As a result, examples of non-mean-field exponents in large N theories are doubly interesting. Moreover some *justification* for their non-mean-field behavior should be given in the sense of [17].

These questions are not only useful for the condensed matter community. The study of phase transitions in large N theories necessarily sheds light on the physics of non-Abelian gauge theories. A general classification of transitions in the phase diagram of such theories is important. Such a dictionary will help in our understanding of QCD-like gauge theories in $(3 + 1)$ dimensions as well as in condensed matter systems in $(2 + 1)$ dimensions. Much is already known. For example, the finite temperature deconfinement transitions of these gauge theories with holographic duals are first order [18] and map onto Hawking-Page [19] phase transitions in the gravity description. Additional transitions have been identified in systems with quarks [20–27]—there are meson-melting transitions in a thermal [28–36] or high-density bath [37–40]. Chiral symmetry is also broken in the system with a magnetic field [41–49] and there is a chiral restoration transition at large densities that occurs in addition to the meson-melting transition. All of these transitions are typically first order at finite temperature and low quark density but continuous at large density (see [50–52] for the full phase diagrams of the D3/D5 and D3/D7 systems with magnetic field which we will study here. For thermodynamics see [53,54]).

Flavored gauge theories are also natural to study from the critical phenomena perspective. Flavor sectors carry new symmetries, leading to a richer phase diagram. At large N, we also get the expansion parameter N_f/N and

*evans@soton.ac.uk
†kristanj@u.washington.edu
‡k.kim@soton.ac.uk

 © 2010 The American Physical Society

so the quenched limit is simultaneously rich and tractable. The holographic description of these theories involves probe D-branes minimizing their worldvolume in the dual geometry [20].

The first example of a holographic quantum critical point separating two nonzero density phases was obtained in the D3/D7 system [50,51]. The dual field theory is simply strongly coupled $\mathcal{N} = 4$ super Yang-Mills (SYM) coupled to a small number of massless fundamental hypermultiplets. The chiral transition in this theory is triggered by large magnetic fields and is second order with mean-field critical exponents. In fact, there are related chiral transitions at nonzero density and magnetic field for almost all of the supersymmetric probe brane systems [55]. Most of these are second-order transitions with mean-field exponents, but a handful are not.

In particular, the first example of a non-second-order, non-mean-field transition in holography was identified in the D3/D5 system [56]. The dual field theory is the same as in the D3/D7 setup, but the flavor fields are confined to a $(2 + 1)$-dimensional defect. The chiral transition in this theory exhibits exponential scaling and so is reminiscent of the celebrated Berezinskii-Kosterlitz-Thouless (BKT) transition [57–59]. This is the first known instance of exponential scaling at zero temperature in $(2 + 1)$ dimensions. Indeed, one of us helped term this new transition a *holographic* BKT transition, as it occurs in a different context than the original BKT transition. Since then holographic BKT transitions have also been found in the context of extremal asymptotically AdS_4 dyonic black holes [60] as well as in two other probe brane setups, namely, flavored Aharony-Bergman-Jaeris-Maldacena theory and flavored (1, 1) little string theory [55,61,62]. They have also been identified in noncritical string setups in [63].

The existence and properties of the BKT transition are intimately related to the Coleman-Mermin-Wagner theorem [64–66]. Recall that transitions of the BKT type are between disordered and *quasiordered* phases in two dimensions. In the quasiordered phase, two-point functions of symmetry-breaking operators have polynomial falloff at long distances while the correlation length in the disordered phases scales as $\exp(c/\sqrt{T - T_c})$ near the critical temperature T_c [58]. Holographic BKT transitions are novel in that they exhibit exponential scaling in an *ordered* phase. Correspondingly, their existence is entirely unrelated to the long-distance restoration of continuous symmetry in two dimensions. On the gravity side, holographic BKT transitions occur due to the violation of the Breitenlohner-Freedman (BF) [67] bound in the infrared region of the dual geometry by a scalar field dual to an order parameter. In the field theory, this amounts to considering a theory with an emergent CFT in the infrared. The transition is driven by taking an operator dimension in the emergent theory into the complex plane. On general grounds presented in [68] this violation was expected to produce BKT scaling, but the D3/D5 system was the first example of a setting where the BF bound is violated controllably.

In all known examples of holographic BKT transitions the dual geometry has an effective infrared AdS_2 region. In the case of extremal asymptotically AdS_4 dyonic black holes, the near-horizon geometry is of the form $AdS_2 \times \mathbb{R}^2$ [9]. For the probe brane systems, there is no physical AdS_2 region at the bottom of the geometry, but worldvolume fields obey the equations of motion for fields in an AdS_2-like region there [69]. For the dyonic black holes the emergent CFT is important: it governs much of the low-frequency form of correlation functions at zero and small temperatures [9]. In this work, the emergent CFT will also be of critical importance.

With all of this background in mind, there is an important open question: can we use the holographic technique to study second-order quantum critical points with non-mean-field exponents?[1] If so, can we explain the exponents at large N? In this work we answer both questions in the affirmative.[2]

Our philosophy is to obtain the most general quantum critical point in a probe brane system (in the strict $N \to \infty$ limit). We do this by considering a theory with three relevant control parameters at zero temperature, one that tends to preserve a symmetry (nonzero density) and the other two to break it (one of them is a magnetic field). Ideally to explore this one should use explicit examples of such a theory. However, the gravitational description of the probe branes is rather restrictive since only a very few operators have their dimensions protected and appear as modes in the Dirac-Born-Infeld (DBI) action of the brane—the rest are stringy modes and have very large dimension. We therefore take a phenomenological approach in this paper and begin with the D3/D5 system at nonzero density and magnetic field. We simply include our third control parameter O into the brane action by hand in a natural fashion. It becomes a magnetic field when its dimension is two and otherwise we tune its dimension. As long as O has dimension less than two,[3] the resulting phase diagram of the theory is quite rich; we plot it in Fig. 1. At fixed density and magnetic field, we find a chiral quantum critical point as we vary O. Varying the magnetic field leads to a line of second-order transitions

[1] At nonzero temperature, there are two known classes for these transitions. In the first, there is a curvature singularity at the transition [70,71]. The second class is phenomenological, where the non-mean-field exponents arise from an effective bulk action [72] whose terms presumably originate from $1/N$ corrections.

[2] As we were finishing this work, the authors of [73] released a paper that studies holographic superfluids in the presence of double-trace deformations. They obtain quantum critical points with non-mean-field scalings that precisely match our results.

[3] When O has a larger dimension than the density, chiral symmetry is broken for any nonzero O as in [41]

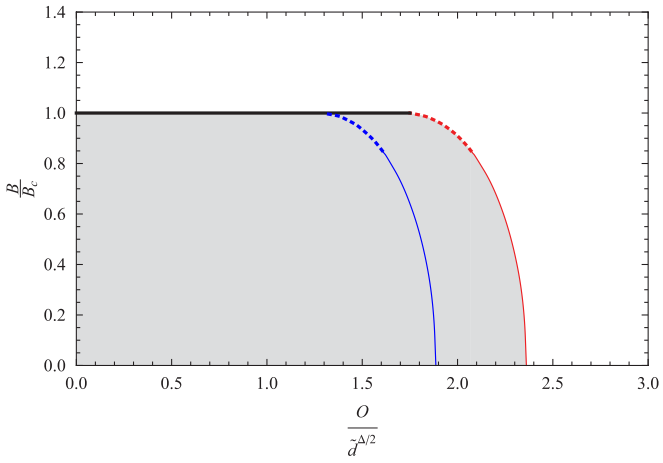

FIG. 1 (color online). The zero temperature phase diagram of our phenomenologically deformed D3/D5 system at nonzero (fixed) density, magnetic field, and simulated control parameter O of dimension Δ. The shaded region indicates the chirally symmetric phase and the white region the broken phase. For $\Delta < 2$, there is a line of holographic BKT transitions at the critical magnetic field $B_c = \tilde{d}/\sqrt{7}$. There is also a line of second-order quantum critical points triggered by O that connects to the line of BKT transitions. The position of the line depends on the precise manner we introduce O. Indeed, the left line corresponds to the choice $\Delta = 5/4$ and the right to $\Delta = 1$. However, the critical exponents are only a function of the magnetic field and density (Fig. 2). The static critical exponent β takes the mean-field value $1/2$ for the solid portion of the lines, but takes on a non-mean-field value for the dotted section as in Eq. (1). The line of critical points then interpolates between a second-order mean-field transition and a holographic BKT transition.

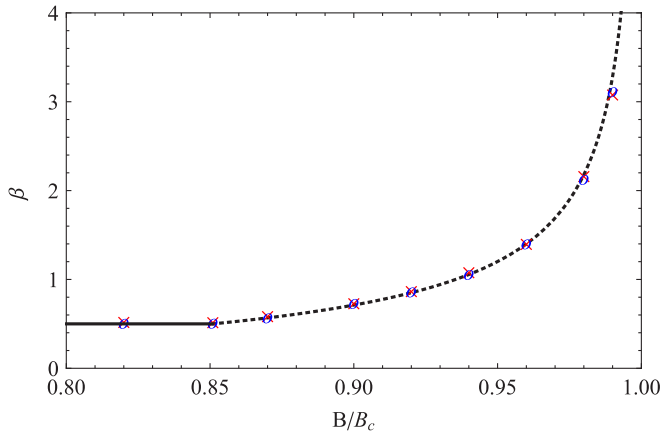

FIG. 2 (color online). The critical exponent β in the deformed D3/D5 system as a function of magnetic field at $\Delta = 1$ and $\Delta = 5/4$. For small magnetic fields—such that $\Delta_{\rm IR} > 3/4$—the exponent β assumes a mean-field value, while for larger magnetic fields it does not. The exponents for $\Delta = 1$ (blue circle) and $\Delta = 5/4$ (red cross) match each other and our prediction (dotted line), Eq. (62), within our numerical accuracy.

that connects to a line of holographic BKT transitions at critical magnetic fields.

In general the exact phase diagram differs depending on our exact choice for the dimension of O. However, the critical exponents of the chiral transition do not. We refer the reader to Figs. 1 and 2, which illustrate these points. This "universality" is one of our central results. In fact, the critical exponents only depend upon the dimension of the scalar field dual to the order parameter in the effective AdS_2 region $\Delta_{\rm IR}$. For example, near the transition the order parameter scales as $\phi \sim (O - O_c)^\beta$, where

$$\beta(\Delta_{\rm IR}) = \begin{cases} \frac{1}{2}, & \Delta_{\rm IR} \in \left[\frac{3}{4}, 1\right), \\ \frac{1-\Delta_{\rm IR}}{2\Delta_{\rm IR}-1}, & \Delta_{\rm IR} \in \left(\frac{1}{2}, \frac{3}{4}\right). \end{cases} \quad (1)$$

In the D3/D5 system, $\Delta_{\rm IR}$ depends on the ratio of magnetic field to density (14)

$$\Delta_{\rm IR} = \frac{1 + \sqrt{\frac{\tilde{d}^2 - 7B^2}{\tilde{d}^2 + B^2}}}{2},$$

where B is the magnetic field and $\tilde{d}$ is proportional to the density. This dimension goes to unity at zero magnetic field and to $1/2$ at the holographic BKT transition $B_c = \tilde{d}/\sqrt{7}$ (from where it then enters the complex plane). This is a nice result: our line of transitions not only exhibits non-mean-field exponents, but it also continuously connects a transition with mean-field exponents at $\Delta_{\rm IR} = 1$ to a holographic BKT transition at $\Delta_{\rm IR} = 1/2$. See also (62).

To understand this interpolation we describe the effective potential of the theory near the line of second-order transitions. We do this numerically, finding that both the order parameter and free energy in the broken phase follow from a modified Landau-Ginzburg model with a potential of the form

$$V_{\rm eff}(\phi) = \alpha_2(O_c - O)\phi^2 + \alpha_4\phi^4 + \alpha_{\rm IR}\phi^{1/(1-\Delta_{\rm IR})}, \quad (2)$$

where the α's are positive couplings and $\Delta_{\rm IR}$ is bigger than $1/2$ and less than 1. When O is tuned past its critical value O_c, the ϕ^4 dominates for $\Delta_{\rm IR} > 3/4$ and the last term dominates for $\Delta_{\rm IR} < 3/4$. In the second regime, the static critical exponent β takes on a non-mean-field value. The nonanalytic term in the potential has a natural form given that there is an emergent $(0 + 1)$-dimensional infrared theory under which the condensate has dimension $1 - \Delta_{\rm IR}$. The term is just that required on dimensional grounds in the infrared theory. We justify this further in Sec. IV.

Our thermodynamic results are obtained numerically. However, we do obtain some analytic results for fluctuations in the symmetric phase of the theory. Following [9], we perform a matching computation to obtain the low-energy limit of the two-point function of the order

parameter. The result for the brane system is essentially the same there. Assuming some basic analyticity constraints, we compute both the correlation length and the dynamical critical exponent near our transitions. The former diverges with mean-field scaling while the latter assumes a non-mean-field value for all nonzero values of the magnetic field. As with β, it only depends on Δ_{IR}.

What happens at nonzero temperature? In the previous examples with both probe branes and holographic superfluids, the transitions are universally second order with mean-field exponents [56]. Even BKT scaling is destroyed at any nonzero temperature. For this reason, we also expect the non-mean-field scaling of our transitions to be lost away from zero temperature. Indeed we find that this is the case below.

Our general conclusion then is that a conformal theory, perturbed by three control parameters O_s, $O_{1,2}$ with dimensions $\Delta_s = \Delta_1 > \Delta_2$ may lead to a phase diagram qualitatively similar to that represented in Fig. 1. In this general picture we require that O_s tends to restore a symmetry and $O_{1,2}$ to break it. The constraint that $\Delta_s = \Delta_1$ amounts to the freedom to change the emergent infrared theory in these systems. Meanwhile, the $\Delta_1 > \Delta_2$ condition allows us to trigger an ordinary second-order transition without altering the infrared theory. Since our results crucially depend upon an emergent CFT, we expect that they extend beyond probe branes to all systems with such an emergent theory.

We further test this picture phenomenologically by performing a similar analysis of the D3/D7 system. In that theory, the magnetic field has dimension two and the baryon density dimension three. We show that if a chiral symmetry-breaking dimension-three operator O is also introduced, then the theory realizes a holographic BKT transition at large O. As in the D3/D5 system, introducing a control parameter with the same dimension as the density leads to an emergent theory where the dimension of a scalar operator depends on the density and O. Moreover, at intermediate O the magnetic field can be used to trigger a second-order non-mean-field transition. While we have not computed it numerically, we expect that the phase diagram qualitatively matches our results for the D3/D5 system.

The outline of this work follows. In Sec. II we review the D3/D5 and D3/D7 systems at nonzero density and magnetic field [50–52,56]. We go on to present our phenomenological models and our holographic regularization. The bulk of our results are presented in Sec. III, beginning with the thermodynamics of the D3/D5 system at zero and nonzero temperature. Next, we study fluctuations using a matching procedure. In Sec. IV we present our effective theory of the transition and critically test it. We apply our analysis briefly to the D3/D7 system without numerics in Sec. V. Finally, we discuss our results in Sec. VI.

II. HOLOGRAPHIC SETUPS

A. The D3/D5 system

Strongly coupled $SU(N)$ $\mathcal{N} = 4$ super Yang-Mills (SYM) theory at large N and zero temperature is dual to type IIB supergravity on $\mathrm{AdS}_5 \times S^5$ (with N D3 branes at its core). The geometry can be written as

$$ds^2 = \frac{w^2}{R^2} dx_{3,1}^2 + \frac{R^2}{w^2}(d\rho^2 + \rho^2 d\Omega_2^2 + dL^2 + L^2 d\bar{\Omega}_2^2), \tag{3}$$

where $w^2 = \rho^2 + L^2$, $d\Omega_2^2$, $d\bar{\Omega}_2^2$ are the metrics for two unit two-spheres, and $R^4 = 4\pi g_s N \alpha'^2$. In these coordinates the Poincáre horizon of AdS is located at $\rho = L = 0$ and the boundary as $\rho^2 + L^2 \to \infty$.

We now add N_f flavor hypermultiplets to the gauge theory along a $(2+1)$-dimensional defect by placing a probe D5 brane in this geometry. The probe limit corresponds to the quenched limit of the gauge theory. The D5 probes are described by their DBI action

$$S_{\mathrm{DBI}} = -N_f T_5 \int d^6\xi \sqrt{-\det(P[G]_{ab} + F_{ab})}, \tag{4}$$

where $a, b = 0, \ldots, 5$ are worldvolume indices, $P[G]_{ab}$ is the pullback of the metric to the brane, and F is the field strength for the diagonal $U(1)$ gauge field living on the D5 worldvolume. The field theory has a $SO(3)_1 \times SO(3)_2 \times U(1)_B$ global symmetry, where the two $SO(3)$'s are chiral R-symmetries and the $U(1)_B$ is a baryon number symmetry which only rotates the flavor fields. The baryon symmetry current is dual to the $U(1)$ gauge field on the brane while the chiral symmetries correspond to the rotational symmetry of the two two-spheres. We now consider an ansatz wherein our brane embeddings are translationally invariant in the wrapped field theory directions x^0–x^2 while wrapping the first two-sphere and the "radial coordinate" ρ. We also consider the theory with no source for the baryon current, that is with $F = 0$. There are then a family of embeddings $L = m$ and x^3, θ_2, ϕ_2 constant (where θ_2, ϕ_2 are coordinates on the unwrapped two-sphere). These are supersymmetric embeddings that correspond to the theory with a hypermultiplet of mass m. The second $SO(3)$ chiral symmetry is then explicitly broken by a hypermass and spontaneously broken by a vacuum expectation value (VEV) for the corresponding operator $\bar{\psi}\psi$ (plus operators related by supersymmetry) [23]. It is this chiral symmetry that is spontaneously broken in our chiral transitions.

We now extend our ansatz to include nonzero baryon density and magnetic field. To do this, we need to let the embedding function L depend on ρ as $L = L(\rho)$ as well as turn on a nontrivial field strength [15,41],

$$F = A_0'(\rho) d\rho \wedge dx^0 + B dx^1 \wedge dx^2, \tag{5}$$

where the field A_0 will determine both the chemical potential and density of baryon charge [37,38,74,75] and B is the magnetic field. The radial electric field A_0' is sourced by charge at the bottom of AdS, and so the brane ends there. This amounts to the boundary condition $L(0) = 0$. For this ansatz we can consistently neglect the Wess-Zumino pieces of the brane action and write

$$S_5 = -\underbrace{N_f T_5 R^6 \mathrm{vol}[S^2]}_{\equiv \mathcal{N}} \mathrm{vol}[\mathbb{R}^{2,1}] \times \int d\rho \rho^2 \sqrt{1 + L'^2 - A_0'^2} \sqrt{1 + \frac{B^2}{w^4}}, \quad (6)$$

where we have defined $w^2 = \rho^2 + L^2$ as well as rescaled x and ρ by powers of R. The normalization is given by $\mathcal{N} = \sqrt{\lambda} N / 2\pi^3$ where $\lambda = 4\pi g_{\mathrm{YM}}^2 N$ is the 't Hooft coupling of the SYM theory. From here onward, we will refer to the action *density* $S_5/\mathrm{vol}[\mathbb{R}^{2,1}]$, describing it with the same notation S_5.

Notably, the action only depends on A_0 through its radial derivative. Thus there is a conserved quantity

$$d = \frac{\delta S_5}{\delta A_0'(\rho, x)} = \frac{\mathcal{N} \rho^2 A_0' \sqrt{1 + \frac{B^2}{w^4}}}{\sqrt{1 + L'^2 - A_0'^2}}. \quad (7)$$

In fact, d is the baryon density in the dual theory. Solving for A_0' in terms of a rescaled density $\tilde{d} = d/\mathcal{N}$, we find

$$A_0'^2 = \frac{\tilde{d}^2 (1 + L'^2)}{\tilde{d}^2 + \rho^4 (1 + \frac{B^2}{w^4})}. \quad (8)$$

We obtain the brane action at fixed density by substituting this result into the action Eq. (6) and Legendre transforming with respect to A_0'. The result is

$$\tilde{S}_5 = -\mathcal{N} \int d\rho \sqrt{1 + L'^2} \sqrt{\tilde{d}^2 + \rho^4 \left(1 + \frac{B^2}{w^4}\right)}. \quad (9)$$

Field configurations $L(\rho)$ that extremize this action correspond to field theory ensembles that extremize the effective potential of the theory in the canonical ensemble. In general, these configurations can only be obtained numerically. However there is an exact solution to the equation of motion for all $\tilde{d}$ and B, $L = 0$, which corresponds to the dual theory with zero hypermass and zero condensate. This solution corresponds to the chirally symmetric phase of the theory.

We continue by reviewing the origin of the chiral BKT transition in this system. The onset of the transition can be understood by studying the stability of the symmetric embedding. Small fluctuations around $L = 0$ are described by the quadratic piece of Eq. (9),

$$\tilde{\mathcal{L}}_5 \sim -\frac{\mathcal{N}}{2} \sqrt{\tilde{d}^2 + B^2 + \rho^4} L'^2 + \frac{\mathcal{N} B^2 L^2}{\rho^2 \sqrt{\tilde{d}^2 + B^2 + \rho^4}}. \quad (10)$$

This Lagrangian has two distinct limits.[4] At large $\rho \gg \sqrt{B}, \sqrt{\tilde{d}}$, the field L/ρ fluctuates as a stable $m^2 = -2$ scalar field in AdS_4. However, at small $\rho \ll \sqrt{B}, \sqrt{\tilde{d}}$, L/ρ fluctuates as a $m^2 = -2B^2/(\tilde{d}^2 + B^2)$ scalar in AdS_2. Thus for $\tilde{d}/B > \sqrt{7}$ the field is stable but for $\tilde{d}/B < \sqrt{7}$ the mass drops below the BF bound [67] in AdS_2, $m_{\mathrm{BF}}^2 = -1/4$. There is therefore a chiral transition at the critical filling fraction

$$\nu_c = \frac{d}{B_c} = \frac{\sqrt{7\lambda} N_f N}{2\pi^3}. \quad (13)$$

Further analysis reveals that the order parameter scales exponentially at smaller densities, so that the transition is of the holographic BKT type. This behavior is the result of the violation of the BF bound in the infrared region which implies that an infinite number of tachyons form at the transition, an extremely unnatural situation within the Landau-Ginzburg-Wilson paradigm. Because it will be important in the rest of this paper, we also note that in the effective AdS_2 region L/ρ is dual to a scalar operator in the emergent CFT of dimension

$$\Delta_{\mathrm{IR}} = \frac{1 + \sqrt{\frac{\tilde{d}^2 - 7B^2}{\tilde{d}^2 + B^2}}}{2}. \quad (14)$$

As usual in AdS/CFT there are two solutions to the equation of motion for the scalar in AdS [see Eq. (12)] which describe an operator in the field theory and its source. The second solution here corresponds to an object of dimension of $1 - \Delta_{\mathrm{IR}}$. We will see below when we discuss the effective theory for our transitions that the three-dimensional condensate corresponds to a dimension $1 - \Delta_{\mathrm{IR}}$ operator in the infrared theory.

At zero magnetic field we have $\Delta_{\mathrm{IR}} = 1$, which decreases to $\Delta_{\mathrm{IR}} = 1/2$ at the transition. In the broken phase, Δ_{IR} is driven into the complex plane. In this way the scaling symmetry of the infrared theory is broken to a discrete subgroup (which is broken further to a self-similar

[4] In our analysis we use the results for a scalar in AdS_{p+1}. The solution of the equation of motion is

$$\frac{L}{\rho} \sim \left(\frac{1}{\rho}\right)^{\Delta}, \quad (11)$$

$$\Delta_{\pm} = \frac{p}{2} \pm \sqrt{\left(\frac{p}{2}\right)^2 + m^2} \quad (12)$$

and the Breitenlohner-Freedman bound [67] is given by $-p^2/4$.

subset by higher energy physics), which relates the various tachyons of the symmetric phase.

B. The D3/D7 system

In the same way we can consider strongly coupled $\mathcal{N} = 4$ SYM at large N coupled to $(3 + 1)$-dimensional fundamental hypermultiplets. In the quenched limit the flavor fields are well described by probe D7 branes in the $AdS_5 \times S^5$ geometry. The global symmetry of this theory is $SO(4) \times U(1)_\chi \times U(1)_B$, where the $U(1)_\chi$ is a chiral symmetry and the $U(1)_B$ is the usual baryon number symmetry. This chiral symmetry is explicitly broken by a hypermass and spontaneously broken by a condensate of the hypermass operator.

On the gravity side, the D7 branes wrap a three-sphere rather than a two-sphere. The $U(1)_\chi$ chiral symmetry is dual to the $SO(2)$ isometry of an $\mathbb{R}^2$ transverse to both stacks of D3 and D7 branes. The baryon symmetry current is dual to the diagonal $U(1)$ gauge field on the D7 branes as before. We then consider a translationally invariant, $SO(4)$-preserving ansatz as before with a density and magnetic field. For such an ansatz the brane action at fixed density is

$$\tilde{S}_7 = -\mathcal{N}_7 \int d\rho \sqrt{1 + L'^2} \sqrt{\tilde{d}^2 + \rho^6 \left(1 + \frac{B^2}{w^4}\right)}. \quad (15)$$

As above, we can study the onset of the chiral transition by studying the stability of small fluctuations around the chirally symmetric embedding $L = 0$. These are described by the quadratic part of Eq. (15),

$$\tilde{\mathcal{L}}_7 \sim -\frac{\mathcal{N}_7}{2} \sqrt{\tilde{d}^2 + \rho^2 B^2 + \rho^6} L'^2 + \frac{\mathcal{N}_7 B^2 L^2}{\sqrt{\tilde{d}^2 + \rho^2 B^2 + \rho^6}}. \quad (16)$$

As with the D3/D5 system, this Lagrangian has two distinct limits. For $\rho \gg \tilde{d}^{1/3}$, $\sqrt{B}$, L/ρ fluctuates as a stable $m^2 = -3$ scalar field in AdS_5. On the other hand, for $\rho \ll \tilde{d}^{1/3}$, $\sqrt{B}$, L/ρ fluctuates as a stable massless scalar in AdS_2. As originally pointed out in [55], there is an emergent CFT in this theory as well. Moreover, L/ρ is dual to a scalar operator in the infrared theory of dimension $\Delta_{IR} = 1$.

There is no holographic BKT transition in this system. Rather, the chiral transition is second order with mean-field exponents. A single tachyon forms at the transition, which is effectively modeled by a Landau-Ginzburg model with a quartic potential. Later, we will see that the mean-field exponents are crucially related to the fact that $\Delta_{IR} = 1$. For the majority of this paper we will work in the D3/D5 system that does have a BKT transition but we will return at the end to produce similar phenomena in a phenomenological deformed version of this D3/D7 system.

C. Phenomenological models

We seek to extend the brane systems above by turning on a third control parameter. For computational simplicity, we seek to deform our setups in such a way that the brane action depends only upon a single worldvolume field and a number of constants of the motion. For the D3/D5 system, there are several candidates. The first is an electric field along the brane [76] and the second a flux on the wrapped two-sphere [77]. Neither deformation breaks chiral symmetry at zero magnetic field and zero hypermass, but the electric field may yet lead to interesting results. Other deformations involve additional worldvolume fields whose equations of motion are not integrable.

In favor of solving a more complicated brane problem with at least two worldvolume fields, we elect to take a phenomenological approach. We will simulate a chiral symmetry-breaking control parameter whose dimension we dial. At first, this approach may seem cavalier: in contrast with the "bottom-up" holographic superfluid and non-Fermi liquid analyses, there are many different ways that control parameters emerge in a probe brane action. There are few *a priori* reasons to believe that phenomenology will accurately predict features of transitions in consistent "top-down" brane setups with three control parameters.

The best justification for our method comes *ex post facto*. Ultimately, we find that the critical exponents we measure do not depend upon the details of our simulated deformation. This result is crucial and we will return to it extensively later. For now, we will simply describe our phenomenological choice. We simulate a control parameter O of dimension Δ (taken to be relevant) in the D3/D5 system by considering a modified brane action

$$\tilde{S}_5 = -\mathcal{N} \int d\rho \sqrt{1 + L'^2} \sqrt{\tilde{d}^2 + \rho^4 \left(1 + \frac{B^2}{w^4} + \frac{O^2}{w^{2\Delta}}\right)}. \quad (17)$$

Note that when O has dimension two, it is effectively a magnetic field.

Earlier we studied both the onset of the chiral transition as well as the emergent infrared theory by studying small fluctuations around the symmetric $L = 0$ embedding. These are now described by the quadratic Lagrangian,

$$\tilde{\mathcal{L}}_5 \sim -\frac{\mathcal{N}}{2} \sqrt{\tilde{d}^2 + B^2 + \rho^{4-2\Delta} O^2 + \rho^4} L'^2 + \left(\frac{B^2}{\rho^2} + \frac{O^2 \Delta}{2\rho^{2(\Delta-1)}}\right) \frac{\mathcal{N} L^2}{\sqrt{\tilde{d}^2 + B^2 + \rho^{4-2\Delta} O^2 + \rho^4}}. \quad (18)$$

This system has two different infrared limits depending upon the value of Δ. For $\Delta > 2$, the new control parameter dominates the infrared, so that L/ρ fluctuates as an unstable scalar there. Then for any nonzero O the symmetric embedding is unstable and the stable phase will break

chiral symmetry. For $\Delta < 2$ the magnetic field and density together dominate the infrared. As before, at small $\rho \ll \sqrt{B}, \sqrt{\tilde{d}}$, the field L/ρ fluctuates as a $m^2 = -2B^2/(\tilde{d}^2 + B^2)$ scalar in an effective AdS_2 region at the bottom of the brane. Finally, the introduction of O tends to break chiral symmetry. We see this by studying small fluctuations at nonzero O but vanishing density and magnetic field. In this limit, the radial equation of motion for the field L/ρ at small ρ is that of a $m^2 = \Delta - 3$ scalar in $AdS_4 - \Delta$. Provided that O is not marginal with $\Delta = 3$, L/ρ fluctuates unstably in the infrared and so the true ground state breaks chiral symmetry as claimed.

We can make a similar phenomenological deformation to introduce an operator O of arbitrary dimension into the D3/D7 system. Just as in the D3/D5 system, we introduce a simulated control parameter into the brane action as

$$\tilde{S}_7 = -\mathcal{N}_7 \int d\rho \sqrt{1 + L'^2} \sqrt{\tilde{d}^2 + \rho^6 \left(1 + \frac{B^2}{w^4} + \frac{O^2}{w^{2\Delta}}\right)}. \tag{19}$$

We will discuss the physics of this model in the later Sec. V.

D. Holographic regularization

The phenomenological brane actions Eq. (17) and (19) contain a number of near-boundary divergences [78]. In a genuine "top-down" construction, these correspond to ultraviolet divergences of the dual theory. In the bulk, they can be diffeomorphism-invariantly regulated by introducing a near-boundary cutoff slice and adding local counterterms on the slice. This process is known as holographic renormalization and is crucial: once we have an appropriately renormalized bulk action, we may sensibly take derivatives to obtain correlation functions.

In our phenomenological constructions, however, we cannot be sure that we diffeomorphism-invariantly regulate the bulk theory. Rather we choose to regularize our theories in a manner inspired by holographic renormalization. We introduce a cutoff slice, add counterterms, and then take the cutoff to infinity. To illustrate the idea, we consider the modified D3/D5 system of Eq. (17), where O has dimension $\Delta = 1$. A general solution $L(\rho)$ has the near-boundary solution

$$L(\rho) = m + \sum_{n=1}^{\infty} \frac{L_n}{\rho^n}, \tag{20}$$

where the L_n for $n > 1$ are recursively determined by m and L_1. The parameter m is simply the hypermass. Then the brane action, integrated up to a cutoff $\rho = \Lambda$, evaluated on such a solution has the near-boundary divergence structure

$$\tilde{S}_{5,\Lambda} = -\mathcal{N} \int d^3x \left(\frac{\Lambda^3}{3} + \frac{O^2 \Lambda}{2}\right) + \text{finite}. \tag{21}$$

The exact divergences depend upon Δ; for $\Delta > 3/4$ there is only a single counterterm required, while for $\Delta = 3/(2n)$ for n a positive integer there is also a logarithmic divergence. These logarithmic divergences correspond to Weyl anomalies of the dual theory [79]. In this case of $\Delta = 1$, we add simple counterterms on the cutoff slice,

$$\tilde{S}_{CT} = \mathcal{N} \int_{\rho=\Lambda} d^3x \sqrt{-\gamma} \left(\frac{1}{3} + \frac{O^2}{2\rho^2}\right), \tag{22}$$

where γ is the induced metric on the slice. When there are logarithmic divergences, we subtract them with counterterms of the form $\sqrt{-\gamma} O^j/(\rho^j \log\rho)$. In general, we define a regularized action by

$$\tilde{S}_{5,\text{reg}} \equiv \lim_{\Lambda\to\infty} [\tilde{S}_{5,\Lambda} + S_{CT}]. \tag{23}$$

We now *define* correlation functions of the dual theory through functional derivatives.

For $\Delta > 1/2$ there are no divergences that depend on m or L_1. Consequently in this region the one-point function of the operator dual to L, the hypermass operator $\mathcal{O}_L$, is simply

$$\phi = \langle \mathcal{O}_L \rangle = -\frac{\delta \tilde{S}_{5,\text{reg}}}{\delta m} = -\mathcal{N} L_1. \tag{24}$$

On the other hand, for $\Delta \leq 1/2$ there are additional contributions to $\langle \mathcal{O}_y \rangle$ that arise from extra L-dependent counterterms. These counterterms are proportional to $L(\rho)^2$ and so lead to a contribution to the condensate proportional to m. These contributions vanish in the chiral limit we consider.

A similar analysis can be performed for the D3/D7 system. Since we do not use the results in this work, we simply quote the highlights. For the choice $\Delta = 3$ that we consider in this work, there are only two divergences: the first corresponds to the infinite volume on the cutoff slice and the second to a logarithmic divergence proportional to $F_{\mu\nu}F^{\mu\nu}$ evaulated on the slice. The regularization is then identical to the holographic renormalization performed in [51]. Notably, the logarithmic divergence corresponds to a Weyl anomaly of the dual theory: the trace of the stress tensor of the dual theory is proportional to F^2.

III. RESULTS

In this section we report the bulk of our numerical results. We begin by studying the zero temperature transitions of our deformed D3/D5 system. As a first numerical check we reproduce the BKT transition in the D3/D5 system with a magnetic field and density. Next, we study this system with the control parameter O present but at zero magnetic field and show that it triggers a mean-field chiral transition. Next, we study the zero temperature phase diagram in the (O, B) plane and identify the line of quantum critical points. We go on to study the nonzero temperature transitions, for which the non-mean-field

scaling is destroyed. Finally we compute the low-energy behavior of the two-point function of the order parameter in the symmetric phase.

A. Zero temperature transitions

1. BKT transition

We begin by studying the D3/D5 system with magnetic field and density to reproduce the BKT transition [56]. To do so we must solve the equation of motion for $L(\rho)$ that follows from varying Eq. (17) with O zero. This equation can be solved numerically. We do so with the shooting method, generally shooting from large ρ.

Recall that the radial electric field on the brane is sourced by charge at the bottom of the geometry. This is equivalent to setting the infrared boundary condition $L(0) = 0$. At small ρ there is then a series solution for L

$$L(\rho) = \gamma_0 + \gamma_1 \rho + \sum_{n=2}^{\infty} \gamma_n \rho^n, \tag{25}$$

where the higher γ_n are recursively determined by γ_0 and γ_1.

Near the AdS_4 boundary we impose the boundary condition that our dual flavor is massless. This amounts to choosing the leading term in the near-boundary solution Eq. (20) to vanish. For our shooting we use the large ρ series solution as initial data (having computed the first dozen or so L_ns) upon which we numerically integrate the corresponding solution to small ρ. We then match this solution onto the small ρ solution. By dialing the field theory condensate we shoot for solutions that extend to the bottom of AdS with $\gamma_0 = 0$. It is numerically difficult to match onto a small ρ series solution. A similar problem emerges in the small ρ embeddings in the flavored little string theory studied in [55]: in each case, there is a nonanalyticity in the equation of motion for L at $\rho = 0$. For the D3/D5 system, embeddings consequently "spike" to $\rho = 0$, infinitely so at infinitesimally small ρ. Nonetheless, with care, we have managed to successfully shoot to the infrared boundary condition with high accuracy.

Generically with large B the solutions bend off the $L = 0$ axis. The chemical potential then forces the solution to spike to the origin at $\rho = L = 0$. At some critical value of B the embeddings smoothly transition to the $L = 0$ embedding. These embeddings are shown in Fig. 3 for varying $B/\tilde{d}$. We also plot the value of the quark condensate c across the embedding to show the BKT exponential scaling.

Note that at yet larger B there is a second transition to a phase with $\tilde{d} = 0$ and stable mesons described by embeddings that curve off the axis but do not spike to the origin. That transition is described for this theory in [52] but we will not explore it further in this paper.

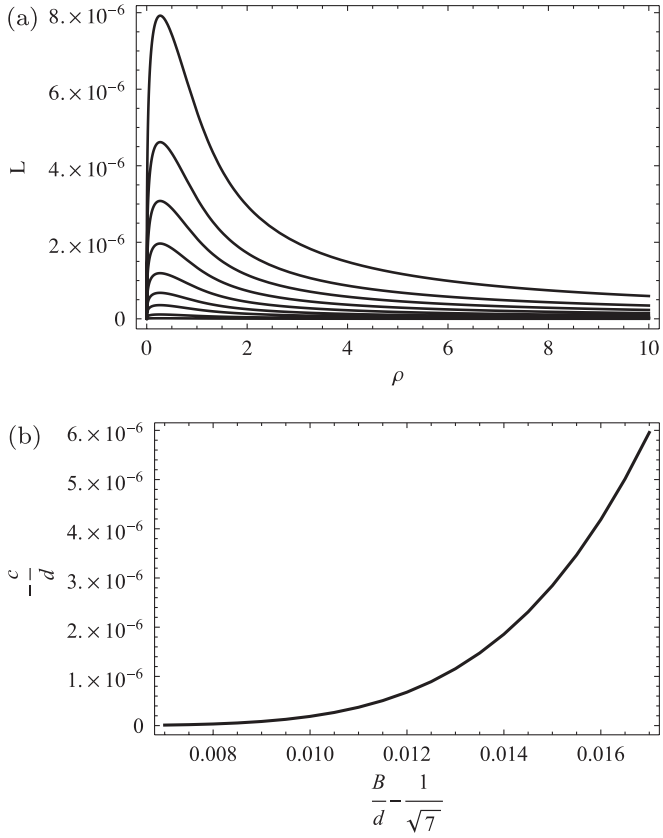

FIG. 3. The BKT transition in the D3/D5 system with quark density and magnetic field present. (a) The embedding L of a D5 brane in the D3 geometry for various $B = \tilde{d}$ showing the BKT transition. (b) A plot of the quark condensate c versus B across the D3/D5 BKT transition.

2. The phenomenological operator O

Next we study the deformed D3/D5 system at zero magnetic field. As we discussed in Sec. II C when the dimension of O is greater than two we find that the chirally broken phase is preferred for all values of the density. This matches the prediction above that the $L = 0$ embedding is unstable for all $\tilde{d}$.

When the dimension of O is less than two, we expect large O at fixed density to trigger a chiral transition. We seek to locate this transition for many different dimensions Δ and to measure the associated critical exponents. To do so we must solve the equation of motion for $L(\rho)$ that follows from varying Eq. (17) with $B = 0$. Again we use the numerical techniques discussed in Sec. III A 1 above.

We find that for large $O \gg \tilde{d}^{\Delta/2}$, the solutions corresponding to zero mass bend away from the symmetric embedding $L = 0$. Near the AdS_4 boundary they necessarily asymptote to the symmetric embedding, but at small ρ they spike to the bottom of AdS. Thus chiral symmetry is indeed broken at large O as expected.

For fixed $\Delta \leq 2$, there is a critical O_c where the embeddings smoothly transition to the symmetric embedding. This is the location of the chiral transition. We locate the

transition for many different Δ, for which we must also scan through O. This is somewhat laborious, as we have to shoot for each value of O and Δ. The net result is shown in Fig. 4. For $\Delta < 2$ we identify a second-order transition with mean-field exponents as promised. At $\Delta = 2$ there is a holographic BKT transition, as O then acts like a magnetic field. We plot the condensate near the transition for the particular case $\Delta = 1$ in Fig. 5 to display that mean-field behavior.

3. The general case

Now we turn on the magnetic field and O together. This will tune the dimension $\Delta_{\rm IR}$ of the operator dual to L/ρ in the emergent theory as we discussed in Sec. II C. As above, we can only solve the equation of motion for L numerically. Our procedure is essentially the same as the one described above in Sec. III A 1.

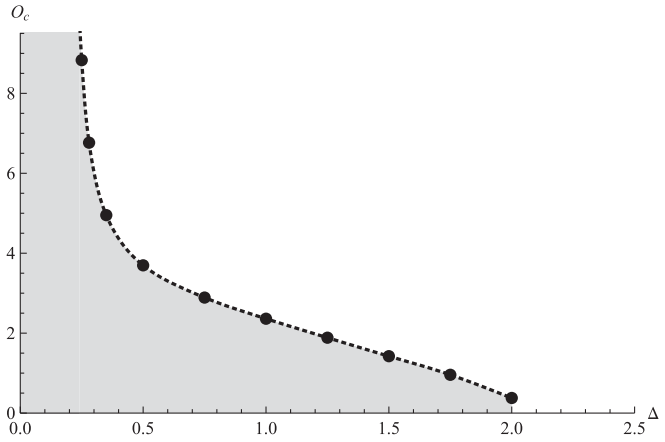

FIG. 4. The zero temperature "phase diagram" of the deformed D3/D5 theory at zero magnetic field as a function of the dimension and value of the deformation O. The shaded region is the chirally symmetric phase and the white is the broken phase. The line of transitions is second-order with mean-field exponents, excepting a holographic BKT transition at $\Delta = 2$.

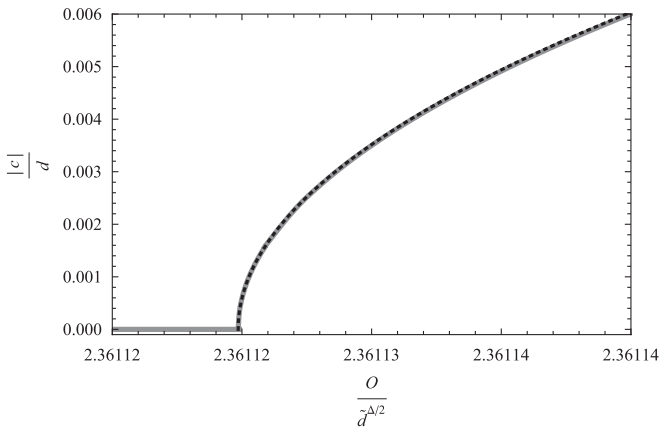

FIG. 5. The condensate in the deformed D3/D5 theory at zero magnetic field and $\Delta = 1$. The solid line is numerical data and the dotted line a fit. Near the transition the condensate scales with a mean-field exponent, $c \sim \sqrt{O - O_c}$.

We studied two different dimensions Δ for O in great detail, $\Delta = 1$ and $\Delta = 5/4$. The choice of a noninteger dimension explicitly shows the independence of our results on that dimension. In each case, we studied the chiral transition at many different magnetic fields and consequently at many values of O as well. For each such choice of O and B we must shoot to find the correct vacuum. As expected, we find a line of second-order chiral transitions. The resulting phase diagram as a function of O and magnetic field was already plotted in Fig. 1. We also plot the critical exponent β as a function of magnetic field in Fig. 2. Recall that β is the scaling of the order parameter in the broken phase, $c \sim (O - O_c)^\beta$.

The combined results are very interesting. First, the line of transitions is second-order as expected. Moreover, for small magnetic fields such that $\Delta_{\rm IR} > 3/4$, the exponent β takes on the mean-field value $1/2$. Once the infrared dimension dips below $3/4$, however, the exponent β is no longer $1/2$ and moreover is independent of the dimension of O. The simplest way to interpret this result is that the effective potential of the theory near the transition has the usual quartic term as well as a second term that depends upon $\Delta_{\rm IR}$ but not Δ. We will show how this occurs explicitly in Sec. IV, where we construct a modified Landau-Ginzburg model for the transition.

B. Nonzero temperature thermodynamics

It is interesting to also study the behavior of our model at nonzero temperature. At nonzero temperature, the $\mathcal{N} = 4$ SYM theory is holographically described by IIB supergravity on an AdS_5 black brane geometry (with N hot D3 branes at its core). The geometry can be written as

$$ds^2 = \frac{w^2}{R^2}(-f(w)(dx^0)^2 + d\vec{x}^2) + \frac{R^2}{f(w)w^2}dw^2 + R^2 d\Omega_5^2, \tag{26}$$

where

$$f(w) = 1 - \frac{w_h^4}{w^2}, \qquad d\Omega_5^2 = d\theta^2 + \cos^2\theta d\Omega_2^2 + \sin^2\theta d\tilde{\Omega}_2^2, \tag{27}$$

and we define $w_h = \pi T/R^2$ with T the temperature of both the field and gravitational theories. This coordinate system is related to the one we employ at zero temperature by $L = w\sin\theta$, $\rho = w\cos\theta$. Both θ and L are dual to the hypermass operator. We change coordinates simply because we have found the numerics easier for this analysis.

As before, we embed N_f D5 branes in this geometry. We consider embeddings that are translationally invariant in the wrapped x^0–x^2 directions, wrap the first two-sphere

and w, and possess no angular momentum on either two-sphere. The embedding is parametrized by the worldvolume field $\theta = \theta(w)$. After adding a charge density and magnetic field, the D5 action at fixed density is

$$\tilde{S}_5 = -\mathcal{N}\int dw\sqrt{1+fw^2\theta'^2}\sqrt{\tilde{d}^2+w^4\cos^4\theta\left(1+\frac{B^2}{w^2}\right)}. \tag{28}$$

Now we add our third control parameter O. There is yet further ambiguity in how we phenomenologically introduce O. We elect to add it in such a way that it again becomes a contribution to the magnetic field when the dimension of O approaches two. Our deformed Lagrangian is

$$\tilde{\mathcal{L}}_5 = -\mathcal{N}\sqrt{1+fw^2\theta'^2}\sqrt{\tilde{d}^2+w^4\cos^4\theta\left(1+\frac{B^2}{w^4}+\frac{O^2}{w^{2\Delta}}\right)}. \tag{29}$$

At zero temperature the holographic BKT transition was triggered by driving the mass of L in the effective AdS_2 region below the BF bound. At any nonzero temperature this exponential scaling is lost [52,56]. The infrared region becomes an AdS_2-like space with a black hole, which has a Rindler near-horizon limit. Driving the mass below the BF bound then corresponds to a UV instability (but not an IR instability) from the point of view of the infrared theory. This instability is tamed by the ultraviolet completion to AdS_4 physics. The absence of such an IR instability presumably leads to the resulting second-order mean-field transition observed at extremely small temperatures in the D3/D5 system.

By the same logic we expect the non-mean-field scaling of our second-order transitions to be destroyed at any nonzero temperature. Indeed, we find this result numerically. To do this, we extremize the modified action Eq. (29) and regularize the bulk action in such a way that we measure the field theory condensate from our embeddings. As at zero temperature, we employ a shooting technique. This time we elect to shoot from the infrared near the black brane horizon. The charge on the brane indicates that the embedding extends down to the horizon. Our infrared boundary condition is then simply that the embedding is regular there.

We plot the condensate near the nonzero temperature transition with small temperature $\pi T = 10^{-5}\sqrt{\tilde{d}}$, magnetic field $B = 0.98B_c$, and the choice $\Delta = 1$ in Fig. 6. At zero temperature and this magnetic field the condensate scales with an exponent $\beta = 2.18$, noticeably different from the mean-field value obtained at the small temperature shown in the figure.

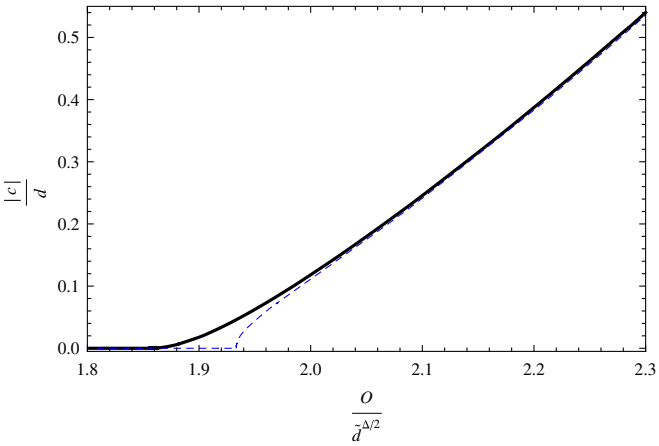

FIG. 6 (color online). The condensate in the deformed D3/D5 system at zero (solid line) and small (dashed line) temperature $\pi T = 10^{-5}\sqrt{\tilde{d}}$, large magnetic field $B = 0.98B_c$, and the choice $\Delta = 1$. The non-mean-field scaling at zero temperature is destroyed even at this small temperature. The nonzero temperature condensate asymptotes to the zero temperature value far away from the transition.

C. Fluctuations

We now move on to consider dynamics. In particular we will obtain the structure of the retarded two-point function of the order parameter at low frequency. This computation essentially mimics the scaling and matching methods employed in [9], so we will only quote the highlights.

We begin by considering a fluctuation of the worldvolume field θ around the symmetric embedding $\theta = 0$. There is an infinite tower of AdS_4 modes corresponding to the Kaluza-Klein harmonics of θ reduced on the wrapped two-sphere; we only consider the s-wave, as this is the lightest mode in the tower. The chiral transition destabilizes it.

After a straightforward, if frustrating, computation we obtain the full Lagrangian for a time and spatially dependent embedding $\theta = \theta(x^0, x^i, w)$. Denoting

$$\theta' = \partial_w\theta, \qquad \dot{\theta} = \partial_{x^0}\theta, \qquad (\nabla\theta)^2 = (\partial_i\theta)(\partial_i\theta), \tag{30}$$

where $i = 1, 2$, we find

$$\tilde{\mathcal{L}}_5 = -\mathcal{N}\sqrt{1+\frac{1+\frac{B^2}{w^4}}{1+\frac{B^2}{w^4}+\frac{(\nabla\theta)^2}{w^2}}\left(w^2f\theta'^2-\frac{\dot{\theta}^2}{w^2f}\right)} \times\sqrt{d^2+w^4\cos^4\theta\left(1+\frac{B^2}{w^4}+\frac{(\nabla\theta)^2}{w^2}\right)}. \tag{31}$$

Now we must choose how to implement our deformation for the system with a spatially varying θ. As before, we make the choice that O becomes a magnetic field for $\Delta = 2$. This amounts to taking

$$\frac{B^2}{w^4} \mapsto \frac{B^2}{w^4} + \frac{O^2}{w^{2\Delta}}. \tag{32}$$

The two-point function of the condensate may be computed by solving the bulk action to second order in the variation. That is, by solving the linearized problem around $\theta = 0$,

$$\mathcal{D}\theta = 0, \tag{33}$$

where $\mathcal{D}$ is a nasty second-order differential operator. We also Fourier transform in the x^μ directions and impose the incoming boundary condition at the horizon. The resulting solution will have a near-boundary expansion

$$\theta = \frac{\theta_1(\omega, k)}{w} + \frac{\theta_3(\omega, k)}{w^3} + O(w^{-4}). \tag{34}$$

Moreover, the two-point function of the condensate is computed by varying the regularized bulk action twice with respect to θ_1,

$$G(\omega, k) = \langle \mathcal{O}(\omega, k)\mathcal{O}(-\omega, -k)\rangle = K\frac{\theta_3(\omega, k)}{\theta_1(\omega, k)}, \tag{35}$$

for K a positive constant. Solving for G at low energies is a bit tricky as the correct infrared behavior of θ depends on ω at leading order. We therefore solve θ in the infrared region and match it to the outer region.

In order to solve for θ near the bottom of the brane we employ a scaling limit. Consider

$$w = \frac{\lambda}{\xi}, \qquad t = \lambda^{-1}\tau, \tag{36}$$

in the $\lambda \to 0$ limit with ξ, τ finite. At zero temperature, the equation of motion of θ becomes that of a $m^2 = -2B^2/(\tilde{d}^2 + B^2)$ scalar field in AdS_2,

$$\partial_\xi^2\theta + \left(\omega^2 + \frac{2B^2}{\tilde{d}^2 + B^2}\frac{1}{\xi^2}\right)\theta = 0. \tag{37}$$

At nonzero temperature, however, we supplement the scaling limit Eq. (36) with

$$w_h = \frac{\lambda}{\xi_0}, \qquad \xi_0 \text{ finite}. \tag{38}$$

The equation of motion in the infrared is then

$$\partial_\xi^2\theta + \frac{\partial_\xi h}{h}\partial_\xi\theta + \left(\frac{\omega^2}{h^2} + \frac{2B^2}{\tilde{d}^2 + B^2}\frac{1}{h\xi^2}\right)\theta = 0, \tag{39}$$

where

$$h = 1 - \frac{\xi_0^4}{\xi^4}. \tag{40}$$

At zero temperature, the scaling limit Eq. (36) amounts to the $\omega \ll \sqrt{\tilde{d}}, \sqrt{B}$ limit. At nonzero temperature Eq. (38) is the $\omega, T \ll \sqrt{\tilde{d}}, \sqrt{B}$ limit with $\omega \sim T$. Notably we can solve for θ in this region at both zero and nonzero temperature. Even more importantly, these equations of motion are (i) independent of both O and its dimension Δ and (ii) those of a scalar in either AdS_2 or an AdS_2 space with a black hole.

Unfortunately the scaling limits Eq. (36) and (38) do not give rise to a systematic matching program. As noted in [9], a proper matching divides the w axis into two regions

$$\text{inner}: w = \frac{\omega}{\xi}, \quad \text{for } \xi \in (\epsilon, \infty), \tag{41}$$

$$\text{outer}: \frac{\omega}{\epsilon} < w, \tag{42}$$

in the limits

$$\omega \to 0, \qquad \xi = \text{finite}, \qquad \epsilon \to 0, \qquad \frac{\omega}{\epsilon} \to 0. \tag{43}$$

Small ω perturbations can be treated systematically in each region, employing ξ as the coordinate in the inner one and r for the outer. The result has the form

$$\text{inner}: \theta_I(\xi) = \theta_I^{(0)}(\xi) + \omega\theta_I^{(1)}(\xi) + \cdots \tag{44}$$

$$\text{outer}: \theta_O(r) = \theta_O^{(0)}(w) + \omega\theta_O^{(1)}(w) + \cdots. \tag{45}$$

The domain of these solutions overlaps in the region defined by $\xi \to 0$ with $w = \omega/\xi \to 0$; the full solution is obtained by matching θ_I and θ_O there.

Now we solve for θ in the inner region. The leading order equation of motion for $\theta_I(\xi)$ is identical to the one we found after the scaling limit, Eq. (39). Near the boundary of the AdS_2 region (that is, $\xi \to 0$), the leading order term in θ_I can be expanded as

$$\theta_I^{(0)}(\omega, k, \xi) = \varphi_+(\xi) + \mathcal{G}_{\Delta_{IR}}(\omega)\varphi_-(\xi), \tag{46}$$

where $\varphi_\pm(\xi)$ are the non-normalizable/normalizable solutions to Eq. (39) and $\mathcal{G}_{IR}(\omega)$ is the retarded Green's function of the operator dual to θ in the infrared theory. It takes on two vastly different forms depending on whether we are at exactly zero or nonzero temperature. For the first, it is [9]

$$\mathcal{G}_{\Delta_{IR}}(\omega) \propto (i\omega)^{2\Delta_{IR}-1}, \tag{47}$$

while at nonzero temperature it is

$$\mathcal{G}_{\Delta_{IR}}(\omega) \propto (i\omega)T^{2\Delta_{IR}-1}. \tag{48}$$

The precise form of $\mathcal{G}$ can be found in [9].

The bottom of the outer region corresponds to the near-boundary region on the infrared AdS_2. The solution to θ_O therefore has the same functional form there, and so we can choose a basis where the linearly independent solutions for θ_O match precisely to $\varphi_\pm$ in the infrared. That is,

$$\theta_O^{(0)}(w) = \eta_+^{(0)}(w) + \mathcal{G}_{\Delta_{IR}}(\omega)\eta_-^{(0)}(w), \tag{49}$$

where $\eta_\pm^{(0)}(w)$ is our (zeroth-order) basis in the outer region. At higher order in ω the matching can be systematically employed, effectively correcting the basis at each order so that

$$\theta_O(w) = \eta_+(w) + \mathcal{G}_{\Delta_{\rm IR}}(\omega)\eta_-(w) \tag{50}$$

is satisfied.

Near the AdS_4 boundary the nth order corrections to $\eta_\pm$ will have an expansion

$$\eta_\pm^{(n)}(w) = \frac{a_\pm^{(n)}(\omega, k)}{w}(1 + \cdots) + \frac{b_\pm^{(n)}(\omega, k)}{w^3}(1 + \cdots). \tag{51}$$

This together with Eq. (35) leads to the desired result, namely, the form of the retarded two-point function

$$G(\omega, k) = K\frac{b_+^{(0)} + O(\omega) + \mathcal{G}_{\Delta_{\rm IR}}(\omega)(b_0^{(0)} + O(\omega))}{a_+^{(0)} + O(\omega) + \mathcal{G}_{\Delta_{\rm IR}}(a_-^{(0)} + O(\omega))}. \tag{52}$$

Moreover, by expanding the a's and b's about $k = 0$, we find that G assumes the small ω, k form

$$G(\omega, k) \sim \frac{g_0 + g_1(i\omega)^{2\Delta_{\rm IR}-1} + g_2k^2}{f_0 + f_1(i\omega)^{2\Delta_{\rm IR}-1} + f_2k^2}, \tag{53}$$

as long as $\Delta_{\rm IR} < 1$. For $\Delta_{\rm IR} > 1$, the low-energy limit is instead

$$G(\omega, k) \sim \frac{\tilde{g}_0 + \tilde{g}_1\omega + \tilde{g}_2k^2}{\tilde{f}_0 + \tilde{f}_1\omega + \tilde{f}_2k^2}. \tag{54}$$

On the reasonable assumption that the matching coefficients, g_i and f_i, are analytic in $O - O_c$, then the chiral transition corresponds to a root in f_0. That is, near the transition f_0 is proportional to $O_c - O$. We then find that for $\Delta_{\rm IR} < 1$ the mode that drives the transition obeys a zero temperature dispersion relation

$$f_1(i\omega)^{2\Delta_{\rm IR}-1} + f_2k^2 \propto O_c - O. \tag{55}$$

From this relation we simultaneously obtain the dynamical critical exponent z at the transition,

$$z = \frac{2}{2\Delta_{\rm IR} - 1}, \tag{56}$$

and the divergence of the correlation length,

$$\langle\phi(x)\phi(0)\rangle \sim e^{-|x|/\xi}, \qquad \xi \sim (O_c - O)^{-\nu}, \qquad \nu = \frac{1}{2}. \tag{57}$$

Thus the dynamical exponent takes a non-mean-field value while ν takes the mean-field one. At nonzero temperature, however, the dispersion relation becomes

$$f_0(i\omega)T^{2\Delta-1} + f_1k^2 = O_c - O, \tag{58}$$

so that the dynamical critical exponent takes on a mean-field value $z = 2$. As with the condensate, the non-mean-field scaling is destroyed at any nonzero temperature.

IV. AN EFFECTIVE MODEL

We have shown that in the D3/D5 system with a magnetic field, density and a phenomenological operator O there is a rich phase structure. The chiral restoration transition is of the holographic BKT type at large B but second order at large O with a region in between with non-mean-field behavior. Our results provide a rich array of numerical data that we will show can be completely matched by a simple effective theory.

Based on [80], we have been able to guess the form of the effective potential. For $\Delta_{\rm IR} > 3/4$, the mean-field scaling of static exponents is reproduced by the potential

$$V_{\rm eff}(\phi) = V_0 + \alpha_2(O_c - O)\phi^2 + \alpha_4\phi^4 + O(\phi^6), \tag{59}$$

where the couplings α_i are presumed to be positive and V_0 is the free energy in the symmetric phase. This generates the expectation value $\phi \sim \sqrt{O - O_c}$. This is just a standard Landau-Ginzburg model.

The crucial ingredient when we move away from mean-field scaling is that the gravity dual reveals that the infrared dynamics is governed by a lower dimensional AdS_{p+1} theory (for the probe brane systems, $p = 1$). We have also learned that the order parameter in this low-energy regime acts as an operator of either dimension $\Delta_{\rm IR}$ or $p - \Delta_{\rm IR}$ [see Eq. (14) for the D3/D5 case]. It is not immediately clear which case holds true; however, we have tried each possibility and find success with our effective model if the dimension of the condensing operator is taken as $p - \Delta_{\rm IR}$.

Now it is natural, on dimensional grounds, to include an additional term in the potential for our order parameter ϕ coming from the p-dimensional theory

$$\Delta V_{\rm eff}(\phi) = \alpha_{\rm IR}\phi^{p/(p-\Delta_{\rm IR})}, \tag{60}$$

Again $\alpha_{\rm IR}$ is assumed to be positive.

If $\frac{3}{4}p < \Delta_{\rm IR} < p$, then the quartic contribution to the effective potential dominates over the term from the infrared theory. In this case, minimizing the potential yields the standard mean-field critical exponent. However, if $\frac{1}{2}p < \Delta_{\rm IR} < \frac{3}{4}p$, then we find the non-mean-field exponent

$$\phi_0 \sim (O - O_c)^\beta \equiv (O - O_c)^{(p-\Delta_{\rm IR}/2\Delta_{\rm IR}-p)}. \tag{61}$$

When the bound $\Delta_{\rm IR} < \Delta_c = 3/4p$ is satisfied, the condensate scales with a non-mean-field exponent.

For the example of the magnetic field competing with our operator O in the D3/D5 system. We can find the expected critical exponent

$$\beta = \frac{1-\Delta_{IR}}{2\Delta_{IR}-1} = \frac{1}{2}\left(\sqrt{\frac{\tilde{d}^2+B^2}{\tilde{d}^2-7B^2}}-1\right), \qquad \left(\sqrt{\frac{3}{29}}\tilde{d} < B < \sqrt{\frac{1}{7}}\tilde{d}\right), \tag{62}$$

where we set $p = 1$ and the B range comes from $1/2 < \Delta_{\rm IR} < 3/4$. As a result $1/2 < \beta < \infty$. For $B < \sqrt{\frac{3}{29}}\tilde{d}$, $\beta = 1/2$. We have plotted the result Eq. (62) over our numerical results in Fig. 2 and they match the numerical results perfectly.

In many ways Eq. (60) is the primary result of this work. The nontrivial emergent theory leaves a fingerprint on the effective potential which can lead to rich phase diagrams even in the strict $N \to \infty$ limit. For example, if $\Delta_{\rm IR} < 5/6$ then a non-mean-field tricritical point is realized by driving either α_4 (for $\Delta_{\rm IR} > 3/4$) or $\alpha_{\rm IR}$ (for $\Delta_{\rm IR} < 3/4$) negative while keeping the other positive. In the first case, the terminating line of second-order transitions has mean-field exponents while in the second it does not.

We can further test our effective potential by measuring the free energy near the transitions we identified in Sec. III A 3, if we write the effective potential as

$$V_{\rm eff}(\phi) = V_0 + \alpha_2(O_c - O)\phi^2 + \alpha_{\rm IR}\phi^{2+(1/\beta)}. \tag{63}$$

In the broken phase this gives

$$\phi \sim (O-O_c)^{\beta}, \qquad \Delta F \sim (O-O_c)^{1+2\beta}, \tag{64}$$

giving a prediction for how the free energy should scale across the transition.

Recall that in order to measure the free energy, we compute (minus) the regularized bulk action. We do this numerically, employing the methods of [51]. We plot some representative results at relatively large magnetic field, $B = 0.95B_c$ and the choice $\Delta = 1$ in Fig. 7. Numerically, we find that the condensate scales with exponent $\beta = 1.20$ and the free energy in the broken phase as $\Delta F/\mathcal{N} \sim -(O-O_c)^{3.38}$. which indeed reproduces the scaling of the free energy for $\beta = 1.20$ to within 1%. We repeated this analysis for many different values of $\Delta_{\rm IR}$ and found the same basic result. The scaling of the free energy is reproduced by the effective potential Eq. (63) for the corresponding exponent β. This shows the strength of the effective potential analysis which does not need to know even the dimension of the operator O.

The effective potential Eq. (60) can be generalized for cases where the emergent theory has different scaling symmetries than in the deformed D3/D5 system. The structure is essentially the same: a Landau-Ginzburg potential analytic in ϕ^2 and a nonanalytic piece stemming from the infrared theory. In the next section we will show such an application to the D3/D7 system.

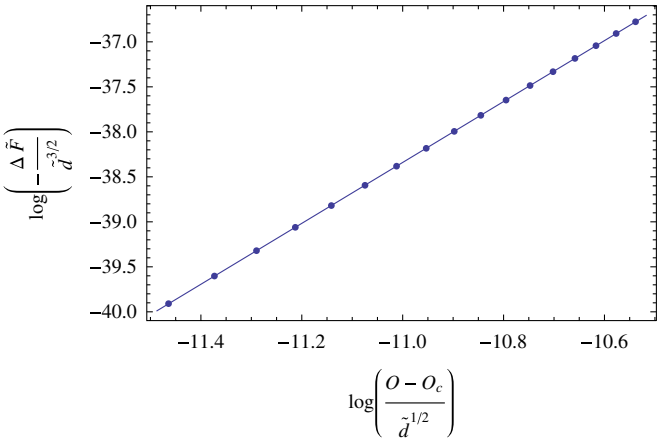

FIG. 7 (color online). A log-log plot of the difference of free energy ΔF in the broken phase at zero temperature as a function of O. The dots indicate numerical data at magnetic field $B = 0.95B_c$ and the choice $\Delta = 1$, and the line a numerical fit. The free energy scales as $\Delta F \sim -(O-O_c)^{3.38}$ in the broken phase.

V. BKT AND NON-MEAN-FIELD TRANSITIONS IN THE D3/D7 SYSTEM

As another example of our phenomenological analysis and effective theory methods let us finally return briefly to the D3/D7 system in Eq. (19). That system has a magnetic field, density, and a phenomenological operator O present.

Looking at linearized fluctuations around the symmetric $L = 0$ embedding, there are three different infrared limits depending on the value of Δ. At large $\Delta > 3$, the field L/ρ fluctuates unstably in the infrared. For $\Delta < 3$, L/ρ fluctuates as a stable massless scalar in AdS_2. However, for the particular case $\Delta = 3$, L/ρ fluctuates as a $m^2 = -3O^2/(\tilde{d}^2+O^2)$ scalar in AdS_2. Adjusting the ratio $O/\tilde{d}$ then tunes the dimension of the scalar operator dual to L in the infrared theory to be

$$\Delta_{\rm IR} = \frac{1+\sqrt{\frac{\tilde{d}^2-11O^2}{\tilde{d}^2+O^2}}}{2}. \tag{65}$$

This last case is perhaps the most interesting. Notably, it corresponds to the case where the density and simulated deformation have the same dimension. As with the D3/D5 system at nonzero magnetic field and density, increasing O at fixed density will trigger a chiral holographic BKT transition at $\tilde{d}/O_c = \sqrt{11}$ as the field L/ρ violates the BF bound in the effective AdS_2 region. On the other hand, at smaller values of O we can presumably drive a second-order chiral transition with the magnetic field. There will be a regime of non-mean-field transitions for some intermediate values of O. The choice $\Delta = 3$ is therefore analogous to our phenomenological D3/D5 system with the roles of the magnetic field and O reversed.

We can apply our effective field theory Eq. (2) to this case too. It predicts the critical exponents

$$\beta = \frac{1}{2}\left(\sqrt{\frac{d^2+O^2}{d^2-11O^2}}-1\right), \qquad \left(\sqrt{\frac{3}{43}}d < O < \sqrt{\frac{1}{11}}d\right). \tag{66}$$

VI. DISCUSSION

We now summarize our results. For our phenomenological D3/D5 setup with magnetic field, density, and a third control parameter we find the nontrivial phase diagram in Fig. 1. The new ingredient is that tuning a third control parameter can lead to a line of second-order transitions. Moreover, the critical exponents of these transitions do not appear to depend on the details of the deformation. Rather they are functions of the dimension Δ_{IR} of the operator dual to the embedding function in an emergent infrared theory. This dimension is tuned by the equal-dimension (in the UV theory) control parameters, density and magnetic field.

We have measured or computed four of the critical exponents along this line. In Sec. III A 3, we numerically measured the condensate in the broken phase and found agreement with an analytic function of the infrared dimension as in Eq. (1). In terms of the magnetic field and density, the exponent β is given by Eq. (62). At smaller $B/\tilde{d}$ (below $\sqrt{3/29}$), β is simply $1/2$. We also computed the free energy in the broken phase and found that both its scaling and β follow from an effective potential Eq. (2). From this we can also compute the critical exponent γ, which is related to the scaling of the susceptibility,

$$\frac{\partial\phi}{\partial m} \sim (O-O_c)^{-\gamma}, \tag{67}$$

since the hypermass m is conjugate to the condensate ϕ. The effective potential with a mass becomes

$$V_{m,\mathrm{eff}}(\phi) = V_{\mathrm{eff}}(\phi) + m\phi. \tag{68}$$

The exponent γ is computed from the effective potential to be the mean-field value $\gamma = 1$.

At nonzero temperature, however, all non-mean-field scaling is lost and the effective potential becomes an ordinary quartic polynomial. The exponents β and γ are $1/2$ and 1, respectively. The temperature destroys the non-mean-field scaling, just as in the holographic BKT transitions.

We also computed the low-energy behavior of the two-point function of the condensate in Sec. III C. Fluctuations of the condensate correspond to time and spatially dependent fluctuations of the bulk field L. At small $w \ll \sqrt{B}$, $\sqrt{\tilde{d}}$, the equation of motion for $\theta \sim L/\rho$ resembles that of a scalar in AdS_2. The equation is solvable there and we match it to the physics outside the infrared region. This enables us to show that at $T = 0$ the dynamical critical exponent is non-mean-field,

$$z = \frac{2}{2\Delta_{\mathrm{IR}}-1},$$

dependent only upon Δ_{IR}. Moreover it returns to the mean-field value $z = 2$ at finite temperature.

In the end, our main results are dependent upon the details of the emergent infrared theory. As a result we expect them to hold in a much wider class of problems, including conformal theories with three control parameters as discussed. It would be nice to test this picture in a purely field theoretic context. In particular, it would be extremely interesting to realize both the emergent theory as well as the sort of phase diagram we identify in a conformal theory without a holographic dual.

ACKNOWLEDGMENTS

K. J. is pleased to thank Andreas Karch and Carlos Hoyos for their insights and conversation. He also thanks Thomas Faulkner for related collaboration to this work. K. J. was supported in part by the U.S. Department of Energy under Grant No. DE-FG02-96ER4095. K-Y. K. was supported by STFC. N. E. is in part supported by STFC and the IPPP.

[1] J. M. Maldacena, Adv. Theor. Math. Phys. **2**, 231 (1998).
[2] E. Witten, Adv. Theor. Math. Phys. **2**, 253 (1998).
[3] S. S. Gubser, I. R. Klebanov, and A. M. Polyakov, Phys. Lett. B **428**, 105 (1998).
[4] D. T. Son and A. O. Starinets, Annu. Rev. Nucl. Part. Sci. **57**, 95 (2007).
[5] C. P. Herzog, A. Karch, P. Kovtun, C. Kozcaz, and L. G. Yaffe, J. High Energy Phys. 07 (2006) 013.
[6] S. S. Gubser, Phys. Rev. D **74**, 126005 (2006).
[7] S.-S. Lee, Phys. Rev. D **79**, 086006 (2009).
[8] M. Cubrovic, J. Zaanen, and K. Schalm, Science **325**, 439 (2009).
[9] T. Faulkner, H. Liu, J. McGreevy, and D. Vegh, arXiv:0907.2694.
[10] S. A. Hartnoll, C. P. Herzog, and G. T. Horowitz, Phys. Rev. Lett. **101**, 031601 (2008).
[11] J. P. Gauntlett, J. Sonner, and T. Wiseman, Phys. Rev. Lett. **103**, 151601 (2009).
[12] S. Sachdev, arXiv:0910.0846.
[13] K. G. Wilson and J. B. Kogut, Phys. Rep. **12**, 75 (1974).
[14] T. Senthil, A. Vishwanath, L. Balents, S. Sachdev, and M. P. A. Fisher, Science **303**, 1490 (2004).
[15] A. Karch and A. O'Bannon, J. High Energy Phys. 11 (2007) 074.

[16] L. G. Yaffe, Rev. Mod. Phys. **54**, 407 (1982).
[17] B. Rosenstein, B. J. Warr, and S. H. Park, Phys. Rev. D **39**, 3088 (1989).
[18] E. Witten, Adv. Theor. Math. Phys. **2**, 505 (1998).
[19] S. W. Hawking and D. N. Page, Commun. Math. Phys. **87**, 577 (1983).
[20] A. Karch and E. Katz, J. High Energy Phys. 06 (2002) 043.
[21] M. Grana and J. Polchinski, Phys. Rev. D **65**, 126005 (2002).
[22] M. Bertolini, P. Di Vecchia, M. Frau, A. Lerda, and R. Marotta, Nucl. Phys. **B621**, 157 (2002).
[23] M. Kruczenski, D. Mateos, R. C. Myers, and D. J. Winters, J. High Energy Phys. 07 (2003) 049.
[24] J. Erdmenger, N. Evans, I. Kirsch, and E. Threlfall, Eur. Phys. J. A **35**, 81 (2008).
[25] A. Karch and L. Randall, J. High Energy Phys. 06 (2001) 063.
[26] O. DeWolfe, D. Z. Freedman, and H. Ooguri, Phys. Rev. D **66**, 025009 (2002).
[27] J. Erdmenger, Z. Guralnik, and I. Kirsch, Phys. Rev. D **66**, 025020 (2002).
[28] J. Babington, J. Erdmenger, N. J. Evans, Z. Guralnik, and I. Kirsch, Phys. Rev. D **69**, 066007 (2004).
[29] R. Apreda, J. Erdmenger, N. Evans, and Z. Guralnik, Phys. Rev. D **71**, 126002 (2005).
[30] T. Albash, V. G. Filev, C. V. Johnson, and A. Kundu, Phys. Rev. D **77**, 066004 (2008).
[31] D. Mateos, R. C. Myers, and R. M. Thomson, Phys. Rev. Lett. **97**, 091601 (2006).
[32] D. Mateos, R. C. Myers, and R. M. Thomson, J. High Energy Phys. 05 (2007) 067.
[33] C. Hoyos-Badajoz, K. Landsteiner, and S. Montero, J. High Energy Phys. 04 (2007) 031.
[34] K. Peeters, J. Sonnenschein, and M. Zamaklar, Phys. Rev. D **74**, 106008 (2006).
[35] J. Erdmenger, M. Kaminski, and F. Rust, Phys. Rev. D **77**, 046005 (2008).
[36] M. Kaminski *et al.*, J. High Energy Phys. 03 (2010) 117.
[37] S. Nakamura, Y. Seo, S.-J. Sin, and K. P. Yogendran, J. Korean Phys. Soc. **52**, 1734 (2008).
[38] S. Kobayashi, D. Mateos, S. Matsuura, R. C. Myers, and R. M. Thomson, J. High Energy Phys. 02 (2007) 016.
[39] S. Nakamura, Y. Seo, S.-J. Sin, and K. P. Yogendran, Prog. Theor. Phys. **120**, 51 (2008).
[40] D. Mateos, S. Matsuura, R. C. Myers, and R. M. Thomson, J. High Energy Phys. 11 (2007) 085.
[41] V. G. Filev, C. V. Johnson, R. C. Rashkov, and K. S. Viswanathan, J. High Energy Phys. 10 (2007) 019.
[42] T. Albash, V. G. Filev, C. V. Johnson, and A. Kundu, J. High Energy Phys. 07 (2008) 080.
[43] V. G. Filev, J. High Energy Phys. 04 (2008) 088.
[44] J. Erdmenger, R. Meyer, and J. P. Shock, J. High Energy Phys. 12 (2007) 091.
[45] A. V. Zayakin, J. High Energy Phys. 07 (2008) 116.
[46] V. G. Filev, C. V. Johnson, and J. P. Shock, J. High Energy Phys. 08 (2009) 013.
[47] V. G. Filev, J. High Energy Phys. 11 (2009) 123.
[48] E. D'Hoker and P. Kraus, J. High Energy Phys. 05 (2010) 083.
[49] E. D'Hoker and P. Kraus, arXiv:1006.2573.
[50] N. Evans, A. Gebauer, K.-Y. Kim, and M. Magou, J. High Energy Phys. 03 (2010) 132.
[51] K. Jensen, A. Karch, and E. G. Thompson, J. High Energy Phys. 05 (2010) 015.
[52] N. Evans, A. Gebauer, K.-Y. Kim, and M. Magou, arXiv:1003.2694.
[53] M. C. Wapler, J. High Energy Phys. 01 (2010) 056.
[54] M. C. Wapler, J. High Energy Phys. 05 (2010) 019.
[55] K. Jensen, Phys. Rev. D **82**, 046005 (2010).
[56] K. Jensen, A. Karch, D. T. Son, and E. G. Thompson, Phys. Rev. Lett. **105**, 041601 (2010).
[57] J. M. Kosterlitz and D. J. Thouless, J. Phys. C **6**, 1181 (1973).
[58] J. M. Kosterlitz, J. Phys. C **7**, 1046 (1974).
[59] V. L. Berezinskii, Zh. Eksp. Teor. Fiz. **59**, 907 (1970).
[60] N. Iqbal, H. Liu, M. Mezei, and Q. Si, Phys. Rev. D **82**, 045002 (2010).
[61] S. S. Pal, arXiv:1006.2444.
[62] O. Aharony, O. Bergman, D. L. Jaeris, and J. Maldacena, J. High Energy Phys. 10 (2008) 091.
[63] U. Gursoy, arXiv:1007.0500; arXiv:1007.4854.
[64] S. R. Coleman, Commun. Math. Phys. **31**, 259 (1973).
[65] N. D. Mermin and H. Wagner, Phys. Rev. Lett. **17**, 1133 (1966).
[66] P. C. Hohenberg, Phys. Rev. **158**, 383 (1967).
[67] P. Breitenlohner and D. Z. Freedman, Ann. Phys. (N.Y.) **144**, 249 (1982).
[68] D. B. Kaplan, J.-W. Lee, D. T. Son, and M. A. Stephanov, Phys. Rev. D **80**, 125005 (2009).
[69] N. Seiberg and E. Witten, J. High Energy Phys. 09 (1999) 032.
[70] A. Karch, A. O'Bannon, and L. G. Yaffe, J. High Energy Phys. 09 (2009) 042.
[71] A. Buchel and C. Pagnutti, Nucl. Phys. **B834**, 222 (2010).
[72] S. Franco, A. M. Garcia-Garcia, and D. Rodriguez-Gomez, Phys. Rev. D **81**, 041901 (2010).
[73] T. Faulkner, G. T. Horowitz, and M. M. Roberts, arXiv:1008.1581.
[74] K.-Y. Kim, S.-J. Sin, and I. Zahed, in *Proceedings of the 2006 International Workshop, Nagoya, Japan, 2006* (World Scientific, Singapore, 2006).
[75] K.-Y. Kim, S.-J. Sin, and I. Zahed, J. High Energy Phys. 01 (2008) 002.
[76] A. Karch and A. O'Bannon, J. High Energy Phys. 09 (2007) 024.
[77] R. C. Myers and M. C. Wapler, J. High Energy Phys. 12 (2008) 115.
[78] A. Karch, A. O'Bannon, and K. Skenderis, J. High Energy Phys. 04 (2006) 015.
[79] M. Henningson and K. Skenderis, J. High Energy Phys. 07 (1998) 023.
[80] K. Jensen and T. Faulkner (unpublished).